Insights into the Structure of Amyloid Fibrils

Karen E. Marshall and Louise C. Serpell*

Department of Biochemistry, John Maynard Smith Building, School of Life Sciences, University of Sussex, Falmer, East Sussex, BN1 9QG, UK

Abstract: Various proteins and peptides are able to self assemble into amyloid fibrils that are associated with disease. Structural characterisation of these fibres is limited by their insoluble and heterogeneous nature. However, advances in various techniques including X-ray diffraction, cryo-electron microscopy and solid state NMR have provided detailed information on various amyloid fibrils, from the long range order and macromolecular structure to the atomic interactions that promote assembly and stabilise the amyloid core. The cross-β model has been widely accepted as a generic structure for most amyloid fibrils and is discussed in detail. It is clear, however, that polymorphisms are present, even in fibrils formed from the same precursor protein, and that these may represent differences in packing at a molecular level. To fully understand the roles of particular residues in amyloid formation and structure, short peptides can be used in conjunction with mutagenesis studies to assess their effects. The structural insights gained using a combination of techniques to study both full-length, disease related peptides and short fragments are essential if progress is to be made towards understanding why these fibres form and how to prevent their formation.

Keywords: Amyloid, structure, X-ray fibre diffraction, Solid State NMR, cross-β.

INTRODUCTION

The observation of amyloid fibril accumulation in different diseases including Alzheimer's Disease (AD), Type II diabetes and Creutzfeldt-Jakob Disease has been well established for a number of years, yet our understanding of the molecular mechanism of these diseases and the exact nature of the pathogenic species remains elusive. Burgeoning evidence suggests that small oligomers are responsible for toxicity [1-8] but their transient and dynamic nature makes them difficult to study. Understanding of the structure of amyloid is fundamental if agents are to be designed to combat amyloid formation, deposition and toxicity, and most progress in the structural characterisation of amyloid has been made on fully formed amyloid fibrils of the type shown in Fig. (**1**). Furthermore, determining how proteins with vastly differing amino acid sequences fold (or "misfold") from their native state to form amyloid fibres with very similar structures could help unravel the mystery of protein folding.

Defining Amyloid

Classically, amyloid is defined by three criteria: the appearance of straight, long and unbranching fibrils approximately 10 nm in width by electron microscopy (EM) (Fig. **1**), an apple green colour when viewed under cross polarised light after staining with the dye Congo Red and a cross-β pattern produced from X-ray fibre diffraction (Fig. **2**). The characteristic cross-β reflections were first seen in X-ray diffraction patterns produced from the egg-stalk of the lacewing *Chrysopa* [9], and subsequently from amyloid obtained from patients with amyloidosis [10]. There are two

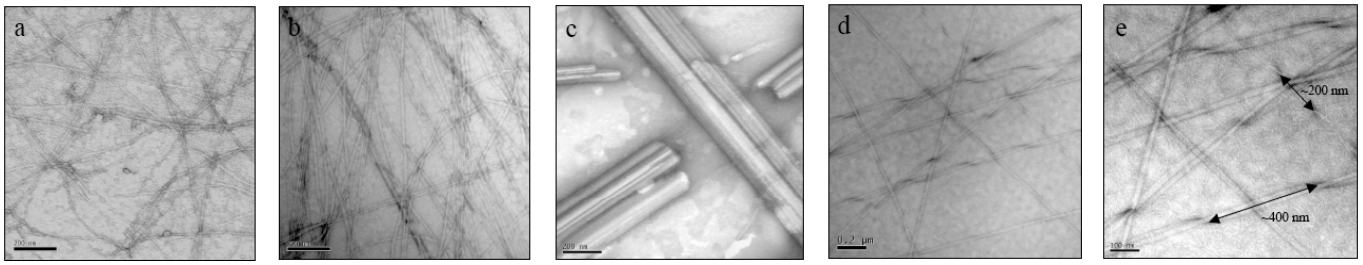

Fig. (1). Transmission electron microscopy of amyloid fibrils showing various morphologies. **a**) Aβ42 formed *in vitro* from synthetic peptide dissolved in water. **b**) Fibrils formed from a small peptide (Ac-KFFEAAAKKFFE-NH2) in water. Note the similarity in overall morphology between the disease related and designed peptide. **c**) Microcrystals formed from the peptide GNNQQNY used for single crystal diffraction to produce the model in Figs. (**3h** and **3i**). **d**) Fibrils formed from the peptide KFFEAAAAKFFE in water. **e**) A higher magnification of image d. There is a regular twist that varies in length (e). The width of the fibrils is around 15nm; 2 of these twist around each other.
Scale bars a-d) = 200 nm, e) =100 nm.

*Address correspondence to this author at the Department of Biochemistry, John Maynard Smith Building, School of Life Sciences, University of Sussex, Falmer, East Sussex, BN1 9QG, UK; Tel: +44 1273 877363; Fax: +44 1273 678433; E-mail: L.C.Serpell@sussex.ac.uk

1874-1967/09

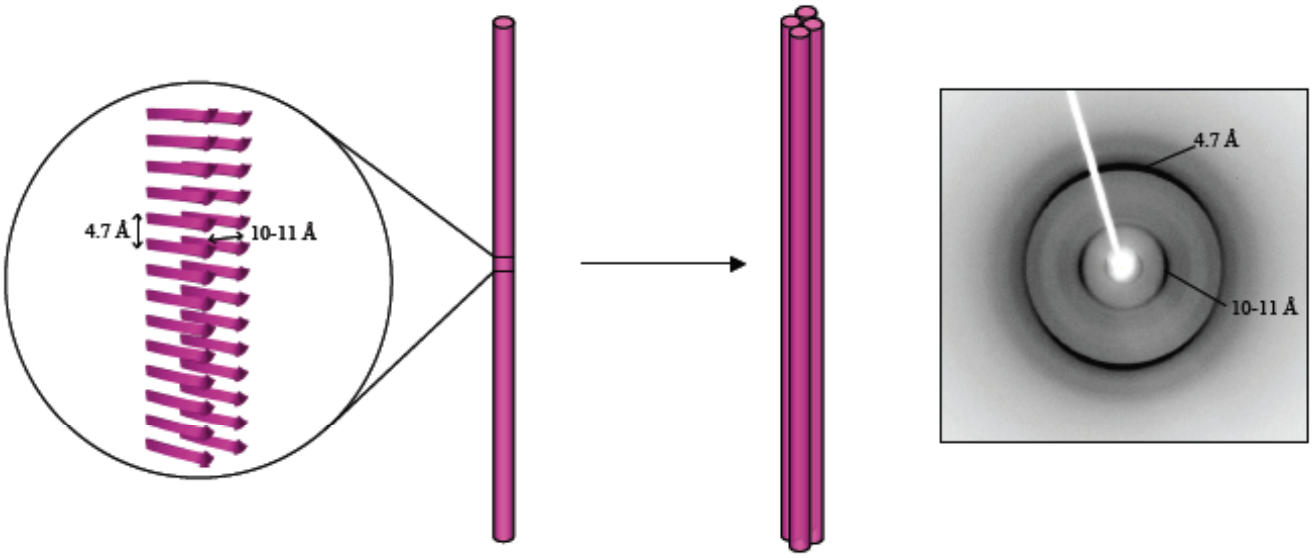

Fig. (2). A schematic of parallel β-strands arranged perpendicular to the fibre axis in a cross-β arrangement, the assembly of protofilaments into mature fibrils and a classical X-ray fibre diffraction pattern showing the 4.7-4.8 Å meridional and 10-11 Å equatorial reflections that define the basic cross-β structure.

notable reflections, a meridional at 4.7-4.8 Å that arises from the spacing between hydrogen bonded β-strands and an equatorial between 10 Å and 11 Å that occurs from the distance between the β–sheets and varies depending on which side chains are present (Fig. **2**) [11]. This arrangement of β-strands perpendicular to the fibre axis has been observed for many different amyloid forming proteins and peptides and suggests a common underlying structure for all amyloid fibrils [12]. In addition to these criteria, there are other indicators of amyloid presence that include fluorescence upon binding the dye Thioflavin T and a peak at around 1620 by Fourier transform infrared spectroscopy (FTIR) indicating presence of β-sheet [13].

Alternative models have been suggested to represent amyloid structure including the water filled nanotube [14], the solenoid or β-helix based structures [15-17] and the stacking of native structures to form fibrils [18]. In this review, we shall concentrate on the cross-β structure as it is the most well studied and representative generic structure of amyloid to date.

Structural Characterisation of Amyloid Fibrils

The ability of many different proteins to form amyloid has led to the search for underlying sequence features that may be responsible for fibril formation, and may therefore be potential therapeutic targets. Whilst the structural characterisation of amyloid formed from disease related proteins or peptides e.g. Amyloid β (Aβ), Islet amyloid polypeptide (IAPP), α-synuclein and transthyretin, may be more clinically relevant, the fibres formed, in particular from *ex-vivo* samples, are often too large and heterogeneous to be studied by the available techniques. Analysing data can be complicated, so instead short segments of known amyloid forming peptides can be used to carry out structural analyses. Often these fragments are from disease-related proteins e.g. KLVFF from Aβ, and sometimes they are designed e.g. KFFEAAAKKFFE [19]. Short sequences such as these retain the ability to form amyloid with similar structural characteristics to their full-length counterparts and their assembled structures can be investigated both experimentally and *in silico* [20-22]. Prediction algorithms have been developed that use primary sequence properties to identify likely β-sheet forming candidates [23-25]. These model systems that form amyloid fibres *in vitro* are much more amenable to structural characterisation by biophysical techniques and can provide more detailed information on the roles of particular residues. The relevance of results obtained on amyloid fibrils *in vitro* compared to those deposited in disease has been supported by FTIR experiments on *in vitro* and *ex vivo* samples of β_2-microglobulin, which both gave similar absorbance maxima [26].

The heterogeneous and insoluble nature of amyloid fibrils has in most cases precluded them from high-resolution structural studies. However, using a combination of techniques it is possible to gain insights into the internal substructure of amyloid at an atomic level and determine the packing arrangements of particular residues. For example, a combination of results from hydrogen deuterium (HD) exchange NMR, mutagenesis and solid-state NMR (ssNMR) concluded that the 3D structure of Aβ42 and Aβ40 amyloid fibrils consisted of two β-sheets (residues 18-26 and 31-42) joined by a β-turn [27, 28] (Fig. **3**, **a-c** and **d-f**). This review will focus on our current knowledge of the cross-β structure of mature amyloid fibrils and their underlying polymorphisms, the various techniques used to gather information and how deeper insight can be gained into the atomic interactions that appear to contribute to and stabilise the amyloid core.

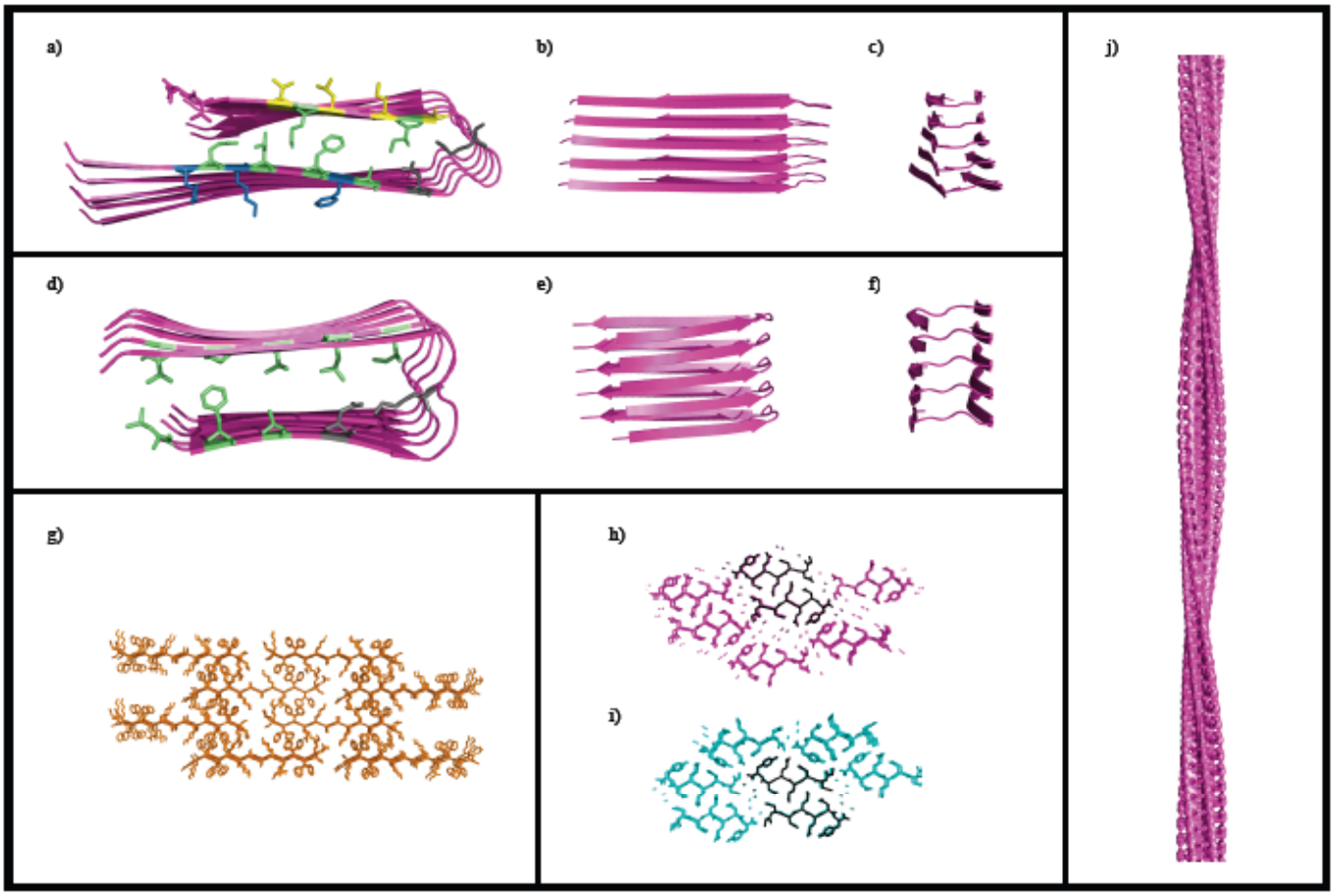

Fig. (3). Some structural models of amyloid fibrils. **a**) view down the fibre axis, **b**) side on to the fibre axis and **c**) at the end of the fibre axis of Aβ40 [69]. Those side chains that interact in the hydrophobic core are shown in green, those that form the hydrophobic face are in yellow, residues on the opposite face are in blue and the D23 and K28 residues that from a salt bridge are in grey. **d**) down, **e**) side and **f**) end views of Aβ42 [27]. The residues that are thought to stabilise the core via hydrophobic interactions are in green and the residues that compose the salt bridge are in grey (D23 and K28). This structure differs to the structure for Aβ40 in that the pairings are inter- rather than intra-molecular. **g**) The side chain packing from the designed amyloid-forming peptide KFFEAAAKKFFE, of particular note are the interactions between Phe residues, likely to be involved in π-π stacking [19]. A fragment from the yeast prion protein Sup35, GNNQQNY, as determined by X-ray crystallography in form 1, **h**) and form 2, **i**), in both forms the sheets interdigitate in the same way in the dry interface (as indicated by the black molecules) [65, 66]; the differences lie in the arrangement of molecules in the wet interface. **j**) The macromolecular structure of β_2-microglobulin fibrils as determined by cryo-EM showing protofilaments twisting around each other [30, 33].

STRUCTURAL HIERARCHY OF AMYLOID FIBRILS

Definitions

Mature amyloid fibrils of the type discussed in this review are thought to assemble in a hierarchical manner and consist of laterally associated smaller protofilaments (Fig. **2**). These protofilaments should not be confused with the smaller proto*fibrils* that are seen in the early stages of amyloid assembly and are thought to contribute to toxicity. Petkova *et al*. assigned definitions to each level in the structural hierarchy of amyloid fibrils that differ somewhat from their globular precursors [29]. As there are no α-helical regions in amyloid core, the secondary structure is limited to β-strands and other regions e.g. loops or bends. The tertiary structure of amyloid is the alignment of β-strands into parallel or antiparallel β-sheets, and the quaternary structure is the arrangement of the sheets with respect to each another [29]. At least two sheets form the protofilaments that can then interact at a higher level to form mature fibres. This macromolecular association and overall morphology can be affected by solution conditions.

The Macromolecular Structure of Amyloid

Cryo-electron microscopy (Cryo-EM) combined with single particle analysis has provided a wealth of information on the macromolecular structure of amyloid fibrils and transmission electron microscopy produces images in which different fibril morphologies are easily observable (Fig. **1**). In its native state insulin is almost entirely α-helical but under denaturing conditions was observed to form amyloid fibrils composed of 2, 4 and 6 relatively flat protofilaments (Table **1**) [30]. Using similar methodologies it was shown that *ex-vivo* lysozyme fibrils and fibres formed from an SH3 domain were composed of 6 and 4 protofilaments respectively [31, 32]. Recently, the cryo-electron microscopy structure of β_2-microglobulin amyloid fibrils has been described, showing a complex arrangement of protofilaments twisting around one another, formed from globular units [33]

Table 1. Methods Used to Determine Some Amyloid Structures (Shown in Fig. 3) Showing Key Structural Features

Peptide	Techniques Used to Determine Structure	Key Features	Side Chain Contacts	Reference
Aβ 1-40 (a-c)	Solid State NMR	Parallel, in register Residues 1-10 disordered Residues 12-24 βstrand 1 Residues 25-29 βturn Residues 30-40 βstrand 2	Residues Q15, L17, F19, A21, I31, M35, V39 in the same molecule interdigitate. A30, I32, L34, V36 and V40 form a hydrophobic face. Residues H14, K16, F20 are on the opposite face. D23 and K28 form a salt bridge.	Petkova PNAS 2002
Aβ1-42 (d-f) (pdb code: 2beg)	HD exchange NMR Mutagenesis	Parallel, in register Residues 1-17 disordered Residues 18-26 βstrand 1 Residues 27-20 βturn Residues 31-42 βstrand 2	Residues L17, F19 and A21 of βstrand 1 on the nth molecule interdigitate with I32, L34, V36, G38 and V40 in βstrand 2 in the (n-1)th molecule. D23 and K28 form a salt bridge.	Luhrs PNAS 2005
KFFEAAAKKFFE (g) (designed peptide)	X-ray fibre diffraction Electron diffraction	Antiparallel sheets	Pi-stacking (Phe) Salt bridges (E and K)	Makin PNAS 2005
GNNQQNY from the yeast prion Sup35 (h and i) (pdb code: form 1 1yjp, form 2 2omm)	X-ray crystallography	Parallel, in register Class 1 steric zipper; pair of β sheets with a dry interface	N2, Q4, N6 interdigitate in the dry interface Amide stacks (Asn) Tyrosine stacks	Nelson Nature 2005 Sawaya Nature 2007
Insulin (j)	Cryo-EM	Long-range interactions between protofilaments, helical twisting	N/A	Jimenez PNAS 2002

(Fig. **3j**). Transthyretin amyloid fibrils from patients with familial amyloidotic polyneuropathy type I were shown by electron microscopy to have cross-sections with a width of around 110 Å-130 Å and are composed of four protofilaments of around 40 Å-50 Å each [34]. Analysis of the images of several fibrils including D67H variant lysozyme, Amyloid A protein and immunoglobulin light chain all showed an electron lucent core [35]. Cryo-EM analysis on Aβ42 and on Aβ40 fibrils revealed two protofilaments winding around a hollow core [36, 37], a feature that has been observed previously in a variety of *ex vivo* and synthetic fibrils [32, 35, 38]. Electron microscopy, magic angle spinning NMR and X-ray fibre diffraction on fibrils formed from residues 105-115 of transthyretin revealed that the protofilaments had an average width of 4.3 nm. Mature fibrils were 10.8 nm, the average length of each peptide was 3.4 nm and the average distance between sheets was 1 nm, leading to the conclusion that protofilaments were composed of 4 β-sheets in a extended conformation and 4 protofilaments wind around each other to form the mature fibrils [39]. α-synuclein fibrils formed either straight (wild type) or twisted (residues 30-110) fibrils that in both cases were composed of two protofilaments, as determined by solid state NMR measurements and cryo-EM [40]. Twisting within mature amyloid fibrils is commonly observed [32, 33, 41]. It is clear that the number of protofilaments involved in a mature amyloid fibril and the overall morphology can vary, even between fibrils formed from the same precursor protein [41, 42].

Polymorphisms within Amyloid

The apparent structural polymorphisms observed in fibrils formed from the same precursor protein may be generated by changing the *in vitro* growth conditions, or they can occur spontaneously. Aβ40 was grown both with and without agitation and produced fibrils that are structurally distinct at the molecular level as determined by ssNMR [43]. Similarly, agitated Aβ40 has been shown to form both flat, striated ribbons that show two-fold symmetry [29] and twisted morphologies that have three-fold symmetry under quiescent conditions with sonication [44]. In both models the β-sheets are parallel and in register, the β-strand and non β-strand regions are very similar and the internal quaternary contacts are almost identical. However, the external quaternary contacts and overall arrangement of the β-strands vary to great extent [44]. A fragment from IAPP appears to take on two forms determined by solid state NMR, one with parallel β-strands in the sheet and the other anti-parallel [45]. The D23N variant of Aβ40, known as the Iowa mutation, was recently investigated using solid state NMR and found to exist in both morphologies with the antiparallel variant predominating [46]. This phenomenon of polymorphism may be related to the existence of prion strains. There are a number of mammalian prion diseases all caused by point mutations in the PrP gene, This leads to the conversion of normally soluble and α-helical PrPc to the β-sheet rich amyloid forming PrPSc and its subsequent self-propagation [47, 48]. Prion strains refer to the different conformations of PrPSc that lead to different phenotypes, yet are all encoded by the same protein [49]. Characterising structural differences between the different prion strains is a challenge. However, using a combination of H/D exchange, solution NMR and mutagenesis, significant differences were found between two strains of the yeast prion Sup35, This work showed that in one conformation a larger proportion of the sequence is involved in the amyloid core [50]. It is generally accepted that the cause of the different disease phenotypes is due to the conformational variation and that a similar

mechanism may apply to non-infectious amyloid diseases [47].

THE CROSS-β MODEL FOR AMYLOID

The cross-β model as a generic structure for amyloid fibrils is historically based upon X-ray fibre diffraction patterns that show the meridional and equatorial reflections similar to those in Fig. (**2**). X-ray fibre diffraction carried out on synthetic Aβ gave a typical cross-β pattern [51-54] as did experiments on *ex vivo* fibrils [55]. Other amyloid fibrils including FAP type I composed of Met 30 variant of transthyretin [56, 57], the amyloidogenic SH3 domain from phosphatidylinositol-3'-kinase [32], lysozyme variants [58], β_2-microglobulin [59] and various amyloidogenic fragments [58, 60-63] have all also shown a cross-β pattern by X-ray diffraction (reviewed in [64]).

Information from other sources also provides evidence for the cross-β arrangement. A fragment from the yeast prion Sup35, GNNQQNY, forms microcrystalline assemblies amenable to single crystal diffraction and was the first example of amyloid structure determination by this method [65]. More recently the Eisenberg group have solved the crystal structures of a number of other short amyloidogenic sequences. However, peptide length appears to be a limitation to this technique, since the peptides that have been solved are seven residues or less [66]. Nevertheless a striking similarity was observed between all the resulting structures. In the the first structure of the GNNQQNY peptide, chains were organised within the fibre in a cross-β conformation in such a way as to generate a steric zipper with a dry interface between sheets and a wet interface between pairs of sheets (Fig. **3 h**, **i** and Table **1**) [65, 66]. Eight classes of steric zipper have been suggested that are thought to account for all amyloid structures, although two have not yet been observed. Advancements in solid state NMR (ssNMR) have provided a high-resolution alternative to X-ray crystallography and the technique has been increasingly applied to structural determination of amyloid with most results supporting the cross-β model. Residues 42-49 of medin, associated with aortic medial amyloid, forms microcrystalline needles that contain parallel, in register strands with contacts between particular residues [60]. Two models have been proposed that are consistent with both ssNMR constraints and fibre diffraction data that vary in the sheet arrangement [60]. Whilst ssNMR can provide structural details at a local level, it is not able to give information on long-range contacts within the same fibre, although recently a supramolecular structure for residues 20-29 of IAPP was deduced by ssNMR [67]. In this model the strands are hydrogen-bonded in an antiparallel arrangement with the sheets being parallel to one another. This contrasts with results from another group that suggest that the same fragment assembles into two forms, one with parallel and the other with antiparallel β strands [45]. There have been more parallel than antiparallel structures published so far [62] but this work again exemplifies the potential for the same sequences to take on different polymorphisms even within the same sample. The fibrillar form of a fragment of β_2-microglobulin has also been investigated using ssNMR, X-ray fibre diffraction and atomic force microscopy and was found to contain β-strand-loop-β-strand monomers stacked up parallel to each other [62]. A model has been proposed for residues 10-35 of Aβ from ssNMR, electron microscopy and small angle neutron scattering that consists of parallel in-register β strands slightly off-set to generate a twist on a macromolecular scale that is observed by EM [68]. Aβ40 did not adopt this same extended conformation and formed a structure with a β-turn with each strand (residues 12-24 and 30-40) stacking up to form parallel β-sheets (Fig. **3 a-c** and Table **1**) [69]. Later work on the same peptide uncovered that different morphologies as viewed by EM and AFM, did not have the same molecular structure (as mentioned previously) and importantly varied in their toxic effects [43]. Aβ42 is thought to adopt a similar conformation with different residues participating in the side-chain interactions (Fig. **3 d-f** and Table **1**) [27].

Electroparamagnetic resonance (EPR) and site directed spin labelling has played a role in determining structural features of amyloid, This provides further evidence that many fibrils contain a cross-β core. It was found that both Aβ40 and Aβ42 contained in-register, parallel structures and could go some way in locating precise residues that were involved in either β-strands, turns or loops, or disordered regions [70]. Subsequent work on α-synuclein fibrils suggested that the core region is formed from residues 36 to 98 but that there are areas within this fragment that are disordered, namely at the start of the NAC (non-amyloid component) region [71, 72]. Perhaps the most significant conclusions from EPR studies on amyloid so far is that an in-register, parallel arrangement of β-strands appears to be the most common structural feature of amyloid, giving further weight to the proposal that cross-β is a representative structure for amyloid [73].

THE MOLECULAR SUBSTRUCTURE OF AMYLOID FIBRILS

As many different proteins and peptides are able to fold into amyloid fibrils it is clear that fibrillisation is not necessarily sequence specific, and it has been proposed that the process is driven purely by backbone interactions [74]. However, interactions between particular residues appear repeatedly in high-resolution structures of amyloid and many are thought to play key aggregational or stabilising roles. The assembly of protofilaments into fibrils is possibly driven by hydrophobic side chains that are exposed on the opposite side to the amyloid core. It is conceivable that the non-specific nature of the hydrophobic interactions between protofilaments could be partly responsible for polymorphisms within amyloid fibres [29, 62]. The stabilisation within the protofilament is thought to arise from side-chain interactions. These may be intra-or inter molecular, for example salt bridges [43] or π-π stacking between aromatic residues in different peptide subunits [11, 19, 62, 75]. Electron and X-ray diffraction were combined to examine the assembled structure of a designed 12-residue peptide (KFFEAAAKKFFE). The subsequent analysis revealed a model structure in which phenylalanine residues associate both between and within the sheets, probably by π-stacking (Fig. **3g** and Table **1**) [19]. The stabilising role of aromatic residues in amyloid inspired the use of di-phenylalanine in nanomaterials with the subunits stacking up to form hollow nanotubes that can act as a scaffold for the creation of

nanowires [76]. In addition to these intermolecular interactions, the role of asparagine has recently been highlighted in the asparagine ladder. These are aligned polar Asn residues in the interior of the fibre that hydrogen-bond with each other to overcome the energetic disadvantage of being in a hydrophobic environment [62, 65, 77]. A poly-glutamine peptide ($K_2Q_{15}D_2$) formed amyloid-like fibrils [14] and analysis of the X-ray diffraction pattern from a mat-textured sample gave a cross-β structure in which hydrogen-bonding interactions were observed between glutamine side chains [78].

Most recent structural work on amyloid has focussed on the determination of specific interactions at an atomic level and has been aided by technological developments, particularly in ssNMR. Research has been carried out into both Aβ40 and Aβ42 to try and establish exactly which residues contribute to both the core stability and aggregation propensities of the peptides. The β-sheets in the model for Aβ42 are stabilised by side chain interactions between F19 and G38, A21 and V36 and a salt bridge between D23 and K28 (Fig. **3d** and Table **1**) [27, 28]. Solid state NMR and disulphide cross-linking experiments on Aβ40 revealed specific inter- and intra-molecular atomic interactions i.e. internal and external quaternary contacts [29, 79]. Several hydrophobic residues and a salt bridge stabilise one molecule while the presence of glycine at residues 33, 37 and 38 create spaces where I31 and M35 fit, known as the external contacts (Fig. **3a** and Table **1**) [29, 69].

Short fragments of amyloidogenic proteins that form fibres with the same morphological and tinctorial properties of the parent peptide, or sequences designed to form amyloid, can give detailed insights into the atomic interactions in the amyloid core. Single point mutations reveal the roles of individual residues in both the fibrillisation process and maintenance of the overall structure. An alanine scan of a 14 residue fragment of acetylcholinesterase revealed that some residues are essential for amyloid formation, in particular aromatic residues [80]. This study also highlighted the stabilising role of salt bridges. The K3 fragment from β_2-microglobulin formed fibrils that showed a similar structure to the native state i.e. β-strand-loop-β-strand, but importantly residues between Phe 22 and Ser 28 are flipped; in the crystal structure of β_2-microglobulin in its native state F22, N24, Y26 and S28 are on the outside of the structure whereas in the fibrils they are located in the hydrophobic interior [62]. This arrangement would lead to optimal intermolecular packing rather than intramolecular stabilisation [62]. Recently two fragments from IAPP, with sequences NNFGAIL and SSTNVG, were crystallised and used as a basis for a model of IAPP [81]. This work built upon the crystal structures that were determined for a number of other short peptides and were mentioned previously [65, 66]. NNFGAIL did not exhibit the steric zipper structure that was proposed as a generic structure for amyloid; instead the monomers formed closely packed β-sheets that excluded water but whose side chains did not interdigitate [81].

CONCLUSIONS

Whilst there is still some controversy as to the precise details of amyloid formation and structure, the combination of techniques, both high and low resolution can lead to some generic conclusions. There is mounting evidence that the cross-β arrangement of β-strands is the most common structure for amyloid fibrils, although the strands and sheets themselves may be parallel or antiparallel. Furthermore, the same peptide may form protofilaments with different arrangements, and these protofilaments have the ability to associate into mature fibres with varying macromolecular architectures. There is evidence to suggest that these differing morphologies are due to differences on an atomic scale and it has been suggested that in a similar fashion to prion strains, these different conformations could influence their pathologies. Understanding of the individual details for each of the amyloid forming proteins is significant challenge. Rules have been established by using short sequences to identify those residues, or combination of residues that have an increased propensity to form amyloid. Further investigation and development in techniques will provide knowledge on both the detailed differences and underlying structural similarities between amyloid fibrils, how they form in the first instance, how their strength and stability can be exploited and how they can be targeted therapeutically in disease.

ACKNOWLEDGEMENTS

This work is supported by funding from Biotechnology and Biological Sciences research council, UK and the Alzheimer's research trust. The authors would like to thank Dr. Julian Thorpe for valuable technical support for the electron microscope and Kyle Morris, Dr. Thomas Williams and Dr. Violetta Soura for useful discussions and help.

REFERENCES

[1] Kayed R, Head E, Thompson JL, McIntire TM, Milton SC, Cotman CW, Glabe CG. Common structure of soluble amyloid oligomers implies common mechanism of pathogenesis. Science 2003; 300(5618): 486-9.

[2] Lacor PN, Buniel MC, Chang L. Synaptic targeting by Alzheimer's-related amyloid beta oligomers. J Neurosci 2004; 24(45): 10191-200.

[3] Haass C, Selkoe DJ. Soluble protein oligomers in neurodegeneration: lessons from the Alzheimer's amyloid beta-peptide. Nat Rev Mol Cell Biol 2007; 8(2): 101-12.

[4] Glabe CG, Kayed R. Common structure and toxic function of amyloid oligomers implies a common mechanism of pathogenesis. Neurology 2006; 66(2 Suppl 1): S74-8.

[5] Volles MJ, Lansbury PT, Jr. Zeroing in on the pathogenic form of alpha-synuclein and its mechanism of neurotoxicity in Parkinson's disease. Biochemistry 2003; 42(26): 7871-8.

[6] Lue LF, Kuo YM, Roher AE. Soluble amyloid beta peptide concentration as a predictor of synaptic change in Alzheimer's disease. Am J Pathol 1999; 155(3): 853-62.

[7] McLean CA, Cherny RA, Fraser FW. Soluble pool of Abeta amyloid as a determinant of severity of neurodegeneration in Alzheimer's disease. Ann Neurol 1999; 46(6): 860-6.

[8] Hardy J, Selkoe DJ. The amyloid hypothesis of Alzheimer's disease: progress and problems on the road to therapeutics. Science 2002; 297(5580): 353-6.

[9] Geddes AJ, Parker KD, Atkins ED, Beighton E. "Cross-beta" conformation in proteins. J Mol Biol 1968; 32(2): 343-58.

[10] Eanes ED, Glenner GG. X-ray diffraction studies on amyloid filaments. J Histochem Cytochem 1968; 16(11): 673-7.

[11] Fandrich M, Dobson CM. The behaviour of polyamino acids reveals an inverse side chain effect in amyloid structure formation. EMBO J 2002; 21(21): 5682-90.

[12] Makin OS, Serpell LC. Structures for amyloid fibrils. FEBS J 2005; 272(23): 5950-61.
[13] Nilsson MR. Techniques to study amyloid fibril formation *in vitro*. Methods 2004; 34(1): 151-60.
[14] Perutz MF, Finch JT, Berriman J, Lesk A. Amyloid fibers are water-filled nanotubes. Proc Natl Acad Sci USA 2002; 99(8): 5591-5.
[15] Ritter C, Maddelein ML, Siemer AB. Correlation of structural elements and infectivity of the HET-s prion. Nature 2005; 435(7043): 844-8.
[16] Wasmer C, Soragni A, Sabate R, Lange A, Riek R, Meier BH. Infectious and noninfectious amyloids of the HET-s(218-289) prion have different NMR spectra. Angew Chem Int Ed Engl 2008; 47(31): 5839-41.
[17] Govaerts C, Wille H, Prusiner SB, Cohen FE. Evidence for assembly of prions with left-handed beta-helices into trimers. Proc Natl Acad Sci USA 2004; 101(22): 8342-7.
[18] Eneqvist T, Andersson K, Olofsson A, Lundgren E, Sauer-Eriksson AE. The beta-slip: a novel concept in transthyretin amyloidosis. Mol Cell 2000; 6(5): 1207-18.
[19] Makin OS, Atkins E, Sikorski P, Johansson J, Serpell LC. Molecular basis for amyloid fibril formation and stability. Proc Natl Acad Sci USA 2005; 102(2): 315-20.
[20] Hoshino M, Katou H, Hagihara Y, Hasegawa K, Naiki H, Goto Y. Mapping the core of the beta(2)-microglobulin amyloid fibril by H/D exchange. Nat Struct Biol 2002; 9(5): 332-6.
[21] Olofsson A, Sauer-Eriksson AE, Ohman A. The solvent protection of alzheimer amyloid-beta-(1-42) fibrils as determined by solution NMR spectroscopy. J Biol Chem 2006; 281(1): 477-83.
[22] Ippel JH, Olofsson A, Schleucher J, Lundgren E, Wijmenga SS. Probing solvent accessibility of amyloid fibrils by solution NMR spectroscopy. Proc Natl Acad Sci USA 2002; 99(13): 8648-53.
[23] Zibaee S, Makin OS, Goedert M, Serpell LC. A simple algorithm locates beta-strands in the amyloid fibril core of alpha-synuclein, Abeta, and tau using the amino acid sequence alone. Protein Sci 2007; 16(5): 906-18.
[24] Trovato A, Seno F, Tosatto SC. The PASTA server for protein aggregation prediction. Protein Eng Des Sel 2007; 20(10): 521-3.
[25] Lopez de la Paz M, Serrano L. Sequence determinants of amyloid fibril formation. Proc Natl Acad Sci USA 2004; 101(1): 87-92.
[26] Jahn TR, Tennent GA, Radford SE. A common beta-sheet architecture underlies *in vitro* and *in vivo* beta2-microglobulin amyloid fibrils. J Biol Chem 2008; 283(25): 17279-86.
[27] Luhrs T, Ritter C, Adrian M, *et al*. 3D structure of Alzheimer's amyloid-beta(1-42) fibrils. Proc Natl Acad Sci USA 2005; 102(48): 17342-7.
[28] Tycko R. Progress towards a molecular-level structural understanding of amyloid fibrils. Curr Opin Struct Biol 2004; 14(1): 96-103.
[29] Petkova AT, Yau WM, Tycko R. Experimental constraints on quaternary structure in Alzheimer's beta-amyloid fibrils. Biochemistry 2006; 45(2): 498-512.
[30] Jimenez JL, Nettleton EJ, Bouchard M, Robinson CV, Dobson CM, Saibil HR. The protofilament structure of insulin amyloid fibrils. Proc Natl Acad Sci USA 2002; 99(14): 9196-201.
[31] Jimenez JL, Tennent G, Pepys M, Saibil HR. Structural diversity of *ex vivo* amyloid fibrils studied by cryo-electron microscopy. J Mol Biol 2001; 311(2): 241-7.
[32] Jimenez JL, Guijarro JI, Orlova E, Zurdo J, Dobson CM, Sunde M, Saibil HR. Cryo-electron microscopy structure of an SH3 amyloid fibril and model of the molecular packing. EMBO J 1999; 18(4): 815-21.
[33] White HE, Hodgkinson JL, Jahn TR. Globular tetramers of beta(2)-microglobulin assemble into elaborate amyloid fibrils. J Mol Biol 2009; 389(1): 48-57.
[34] Serpell LC, Sunde M, Fraser PE. Examination of the structure of the transthyretin amyloid fibril by image reconstruction from electron micrographs. J Mol Biol 1995; 254(2): 113-8.
[35] Serpell LC, Sunde M, Benson MD, Tennent GA, Pepys MB, Fraser PE. The protofilament substructure of amyloid fibrils. J Mol Biol 2000; 300(5): 1033-9.
[36] Zhang R, Hu X, Khant H. Interprotofilament interactions between Alzheimer's A{beta}1-42 peptides in amyloid fibrils revealed by cryoEM. Proc Natl Acad Sci USA 2009; 106(12): 4653-8.
[37] Sachse C, Fandrich M, Grigorieff N. Paired beta-sheet structure of an Abeta(1-40) amyloid fibril revealed by electron microscopy. Proc Natl Acad Sci USA 2008; 105(21): 7462-6.
[38] Serpell LC, Smith JM. Direct visualisation of the beta-sheet structure of synthetic Alzheimer's amyloid. J Mol Biol 2000; 299(1): 225-31.
[39] Jaroniec CP, MacPhee CE, Bajaj VS, McMahon MT, Dobson CM, Griffin RG. High-resolution molecular structure of a peptide in an amyloid fibril determined by magic angle spinning NMR spectroscopy. Proc Natl Acad Sci USA 2004; 101(3): 711-6.
[40] Vilar M, Chou HT, Luhrs T. The fold of alpha-synuclein fibrils. Proc Natl Acad Sci USA 2008; 105(25): 8637-42.
[41] Goldsbury C, Goldie K, Pellaud J. Amyloid fibril formation from full-length and fragments of amylin. J Struct Biol 2000; 130(2-3): 352-62.
[42] Sumner Makin O, Serpell LC. Structural characterisation of islet amyloid polypeptide fibrils. J Mol Biol 2004; 335(5): 1279-88.
[43] Petkova AT, Leapman RD, Guo Z, Yau WM, Mattson MP, Tycko R. Self-propagating, molecular-level polymorphism in Alzheimer's beta-amyloid fibrils. Science 2005; 307(5707): 262-5.
[44] Paravastu AK, Leapman RD, Yau WM, Tycko R. Molecular structural basis for polymorphism in Alzheimer's beta-amyloid fibrils. Proc Natl Acad Sci USA 2008; 105(47): 18349-54.
[45] Madine J, Jack E, Stockley PG, Radford SE, Serpell LC, Middleton DA. Structural insights into the polymorphism of amyloid-like fibrils formed by region 20-29 of amylin revealed by solid-state NMR and X-ray fiber diffraction. J Am Chem Soc 2008; 130(45): 14990-5001.
[46] Tycko R, Sciarretta KL, Orgel JP, Meredith SC. Evidence for novel -sheet structures in iowa-mutant -amyloid fibrils. Biochemistry 2009; 48(26): 6072-84.
[47] Telling GC, Parchi P, DeArmond SJ. Evidence for the conformation of the pathologic isoform of the prion protein enciphering and propagating prion diversity. Science 1996; 274(5295): 2079-82.
[48] Wickner RB, Edskes HK, Shewmaker F, Nakayashiki T. Prions of fungi: inherited structures and biological roles. Nat Rev Microbiol 2007; 5(8): 611-8.
[49] Weissmann C. Prion diseases. Yielding under the strain. Nature 1995; 375(6533): 628-9.
[50] Toyama BH, Kelly MJ, Gross JD, Weissman JS. The structural basis of yeast prion strain variants. Nature 2007; 449(7159): 233-7.
[51] Kirschner DA, Inouye H, Duffy LK, Sinclair A, Lind M, Selkoe DJ. Synthetic peptide homologous to beta protein from Alzheimer disease forms amyloid-like fibrils *in vitro*. Proc Natl Acad Sci USA 1987; 84(19): 6953-7.
[52] Inouye H, Fraser PE, Kirschner DA. Structure of beta-crystallite assemblies formed by Alzheimer beta-amyloid protein analogues: analysis by x-ray diffraction. Biophys J 1993; 64(2): 502-19.
[53] Malinchik SB, Inouye H, Szumowski KE, Kirschner DA. Structural analysis of Alzheimer's beta(1-40) amyloid: protofilament assembly of tubular fibrils. Biophys J 1998; 74(1): 537-45.
[54] Sikorski P, Atkins ED, Serpell LC. Structure and texture of fibrous crystals formed by Alzheimer's abeta(11-25) peptide fragment. Structure 2003; 11(8): 915-26.
[55] Kirschner DA, Abraham C, Selkoe DJ. X-ray diffraction from intraneuronal paired helical filaments and extraneuronal amyloid fibers in Alzheimer disease indicates cross-beta conformation. Proc Natl Acad Sci USA 1986; 83(2): 503-7.
[56] Terry CJ, Damas AM, Oliveira P. Structure of Met30 variant of transthyretin and its amyloidogenic implications. EMBO J 1993; 12(2): 735-41.
[57] Blake C, Serpell L. Synchrotron X-ray studies suggest that the core of the transthyretin amyloid fibril is a continuous beta-sheet helix. Structure 1996; 4(8): 989-98.
[58] Sunde M, Serpell LC, Bartlam M, Fraser PE, Pepys MB, Blake CC. Common core structure of amyloid fibrils by synchrotron X-ray diffraction. J Mol Biol 1997; 273(3): 729-39.
[59] Smith DP, Jones S, Serpell LC, Sunde M, Radford SE. A systematic investigation into the effect of protein destabilisation on beta 2-microglobulin amyloid formation. J Mol Biol 2003; 330(5): 943-54.
[60] Madine J, Copland A, Serpell LC, Middleton DA. Cross-beta spine architecture of fibrils formed by the amyloidogenic segment NFGSVQFV of medin from solid-state NMR and X-ray fiber diffraction measurements. Biochemistry 2009; 48(14): 3089-99.

[61] Ferguson N, Becker J, Tidow H. General structural motifs of amyloid protofilaments. Proc Natl Acad Sci USA 2006; 103(44): 16248-53.
[62] Iwata K, Fujiwara T, Matsuki Y, Akutsu H, Takahashi S, Naiki H, Goto Y. 3D structure of amyloid protofilaments of beta2-microglobulin fragment probed by solid-state NMR. Proc Natl Acad Sci USA 2006; 103(48): 18119-24.
[63] Steinmetz MO, Gattin Z, Verel R. Atomic models of de novo designed cc beta-Met amyloid-like fibrils. J Mol Biol 2008; 376(3): 898-912.
[64] Makin OS, Sikorski P, Serpell LC. Diffraction to study protein and peptide assemblies. Curr Opin Chem Biol 2006; 10(5): 417-22.
[65] Nelson R, Sawaya MR, Balbirnie M. Structure of the cross-beta spine of amyloid-like fibrils. Nature 2005; 435(7043): 773-8.
[66] Sawaya MR, Sambashivan S, Nelson R. Atomic structures of amyloid cross-beta spines reveal varied steric zippers. Nature 2007; 447(7143): 453-7.
[67] Nielsen JT, Bjerring M, Jeppesen MD. Unique identification of supramolecular structures in amyloid fibrils by solid-state NMR spectroscopy. Angew Chem Int Ed Engl 2009; 48(12): 2118-21.
[68] Benzinger TL, Gregory DM, Burkoth TS. Two-dimensional structure of beta-amyloid(10-35) fibrils. Biochemistry 2000; 39(12): 3491-9.
[69] Petkova AT, Ishii Y, Balbach JJ. A structural model for Alzheimer's beta -amyloid fibrils based on experimental constraints from solid state NMR. Proc Natl Acad Sci USA 2002; 99(26): 16742-7.
[70] Torok M, Milton S, Kayed R. Structural and dynamic features of Alzheimer's Abeta peptide in amyloid fibrils studied by site-directed spin labeling. J Biol Chem 2002; 277(43): 40810-5.
[71] Der-Sarkissian A, Jao CC, Chen J, Langen R. Structural organization of alpha-synuclein fibrils studied by site-directed spin labeling. J Biol Chem 2003; 278(39): 37530-5.
[72] Chen M, Margittai M, Chen J, Langen R. Investigation of alpha-synuclein fibril structure by site-directed spin labeling. J Biol Chem 2007; 282(34): 24970-9.
[73] Margittai M, Langen R. Fibrils with parallel in-register structure constitute a major class of amyloid fibrils: molecular insights from electron paramagnetic resonance spectroscopy. Q Rev Biophys 2008; 41(3-4): 265-97.
[74] Dobson CM. The structural basis of protein folding and its links with human disease. Philos Trans R Soc Lond B Biol Sci 2001; 356(1406): 133-45.
[75] Gazit E. A possible role for pi-stacking in the self-assembly of amyloid fibrils. FASEB J 2002; 16(1): 77-83.
[76] Reches M, Gazit E. Casting metal nanowires within discrete self-assembled peptide nanotubes. Science 2003; 300(5619): 625-7.
[77] Kajava AV, Aebi U, Steven AC. The parallel superpleated beta-structure as a model for amyloid fibrils of human amylin. J Mol Biol 2005; 348(2): 247-52.
[78] Sikorski P, Atkins E. New model for crystalline polyglutamine assemblies and their connection with amyloid fibrils. Biomacromolecules 2005; 6(1): 425-32.
[79] Shivaprasad S, Wetzel R. An intersheet packing interaction in A beta fibrils mapped by disulfide cross-linking. Biochemistry 2004; 43(49): 15310-7.
[80] Jean L, Lee CF, Shaw M, Vaux DJ. Structural elements regulating amyloidogenesis: a cholinesterase model system. PLoS ONE 2008; 3(3): e1834.
[81] Wiltzius JJ, Sievers SA, Sawaya MR. Atomic structure of the cross-beta spine of islet amyloid polypeptide (amylin). Protein Sci 2008; 17(9): 1467-74.

Received: April 21, 2009 Revised: July 07, 2009 Accepted: July 09, 2009